SCIENTIFIC REPORTS

OPEN

SUBJECT AREAS:
STABLE ISOTOPES
STATISTICS
PALAEOCEANOGRAPHY
OCEAN SCIENCES

Received
27 May 2014

Accepted
23 July 2014

Published
11 August 2014

Correspondence and requests for materials should be addressed to K.T. (kau@ig.utexas.edu)

Globigerinoides ruber morphotypes in the Gulf of Mexico: A test of null hypothesis

Kaustubh Thirumalai[1,2], Julie N. Richey[3], Terrence M. Quinn[1,2] & Richard Z. Poore[3]

[1]Institute for Geophysics, Jackson School of Geosciences, University of Texas at Austin, J. J. Pickle Research Campus, Building 196, 10100 Burnet Road (R2200), Austin, Texas 78758-4445, USA, [2]Department of Geological Sciences, Jackson School of Geosciences, University of Texas at Austin, 1 University Station C9000, Austin, Texas 78712-1722, USA, [3]United States Geological Survey, St. Petersburg Coastal and Marine Science Center, 600, Fourth Street South, St. Petersburg, FL 33701-4846.

Planktic foraminifer *Globigerinoides ruber* (*G. ruber*), due to its abundance and ubiquity in the tropical/subtropical mixed layer, has been the workhorse of paleoceanographic studies investigating past sea-surface conditions on a range of timescales. Recent geochemical work on the two principal white *G. ruber* (W) morphotypes, sensu stricto (ss) and sensu lato (sl), has hypothesized differences in seasonal preferences or calcification depths, implying that reconstructions using a non-selective mixture of morphotypes could potentially be biased. Here, we test these hypotheses by performing stable isotope and abundance measurements on the two morphotypes in sediment trap, core-top, and downcore samples from the northern Gulf of Mexico. As a test of null hypothesis, we perform the same analyses on couplets of *G. ruber* (W) specimens with attributes intermediate to the holotypic ss and sl morphologies. We find no systematic or significant offsets in coeval ss-sl $\delta^{18}O$, and $\delta^{13}C$. These offsets are no larger than those in the intermediate pairs. Coupling our results with foraminiferal statistical model INFAUNAL, we find that contrary to previous work elsewhere, there is no evidence for discrepancies in ss-sl calcifying depth habitat or seasonality in the Gulf of Mexico.

The geochemistry of foraminiferal tests from marine sediment is utilized extensively as a tool to infer paleoceanographic variability on timescales ranging from decades to millennia, thereby playing an integral role in our understanding of climate change[1–7]. In reconstructing geochemically derived estimates of paleoceanographic parameters, attention must be paid to the ecology and taxonomy of the foraminifera selected for analysis. Inaccurate identification of species could potentially bias or distort reconstructions and add an unknown dimension of uncertainty to quantitative estimates of paleoceanographic parameters[8,9].

Planktic foraminifer *Globigerinoides ruber* (*G. ruber*) is perhaps one of the most widely used species for reconstructing past sea-surface conditions[1–7]. *Globigernoides ruber* is ubiquitous in the mixed layer of tropical/subtropical waters and is known to live throughout the year[10,11]. Thus, its geochemistry is an attractive proxy for past sea-surface temperature (SST) and $\delta^{18}O$ of seawater ($\delta^{18}O_{sw}$).

Apart from its pink chromotype, *G. ruber* (P), multiple morphotypical variants of its white variety, *G. ruber* (W), have been identified and described in micropalentological literature. These include *Globigerinoides elongatus*[12], *Globigerinoides pyramidalis*[13], *Globigerinoides cyclostomus*[14], and the holotypic normalform of *G. ruber* (W), first described as *Globigerina rubra*[15]. More recently, stable isotopic and trace metal geochemistry studies have placed the former three variants under *G. ruber* sensu lato (sl) while the latter has been termed *G. ruber* sensu stricto (ss), albeit acknowledging a large range of transitional forms between the morphotypes[16–21] (Fig. 1). These studies compared the stable isotopic oxygen and carbon composition of the two morphotypes in core-tops, downcore sediments, and sediment traps from the South China Sea, Indo-Pacific, and Japanese seas[16–21].

Understanding the ecology of modern *G. ruber* (W) sets up the expectation for interpreting signals derived from downcore geochemical variations. Previous studies based on core-tops and downcore samples, despite small sample numbers (5–23 pairs), inferred that differences in stable isotopes were the result of either distinct calcifying depth habitats (ss: ~0–25 m, sl: ~25–50 m), seasonal preferences (sl: winter-biased), or vital effects between *G. ruber* (W) ss and sl, and concluded that the sl morphotype was a cold-biased specimen[16–19]. These results have critical implications for paleoceanographic reconstructions using a non-selective mixture of the two morphotypes, as they can be biased or distorted due to the averaging of signals from different depths or seasons.

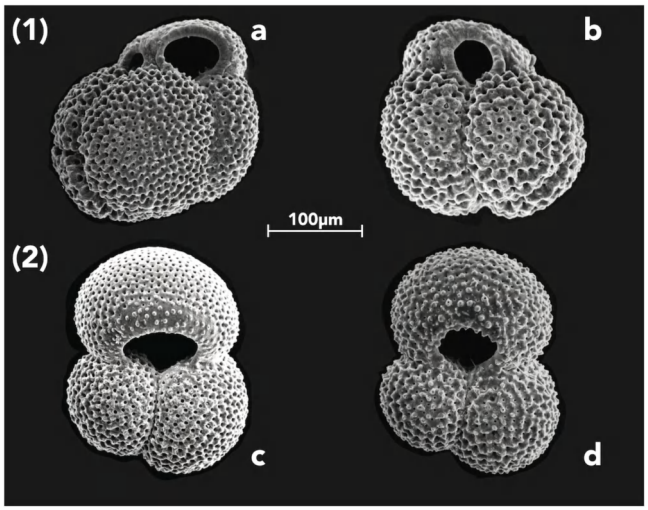

Figure 1 | Scanning Electron Micrographs of *Globigerinoides ruber* (White) morphotypes. (1) a and b: *G. ruber* (W) sensu lato; (2) c and d: *G. ruber* (W) sensu stricto.

The sediment trap studies, where the age of the samples are known with weekly/monthly precision, found little-to-no differences in the stable isotopes[20,21]. Hence it is important to study both the modern ecology and geochemistry of these morphotypes using large sample numbers and different sampling archives in order to quantify the degree of bias that may occur due to morphotypical variability in *G. ruber* (W).

In this work, we study the stable isotopic differences between coeval ss and sl from core-tops, late Holocene downcore samples, and a sediment trap in the northern Gulf of Mexico. As a geochemical test of the null hypothesis, we also analyze mixed *G. ruber* (W) couplets with morphologies intermediate to the ss and sl holotypes (hereafter 'intermediate' *G. ruber* (W) tests) to systematically investigate the composition of different *G. ruber* (W) subsets: if the geochemical composition of all subsets are comparable, we fail to reject the null hypothesis that morphotypical variability has no effect on *G. ruber* (W) geochemistry; if they are consistently different, then we reject the null hypothesis and conclude that morphotypical variability has a significant effect on *G. ruber* (W) geochemistry. We couple these results with INFAUNAL, a recently published foraminiferal statistical model[22], to gain insight into the use of the two morphotypes as paleoceanographic recorders in the Gulf of Mexico.

Results

We report here 130 $\delta^{18}O$ and $\delta^{13}C$ measurements on 37 pairs of *G. ruber* (W) ss and sl along with 28 pairs of intermediate *G. ruber* (W) tests from three sampling archives in the northern Gulf of Mexico (*Supplementary Fig. 1*): core-tops, downcore samples, and a sediment trap (Fig. 2 and 3). Table 1 lists the mean and standard deviation of ss-sl measurements in each archive. Here, the mean and standard deviation reflect the overall (time-dependent) variability in our selected samples of each archive; for example, sediment trap standard deviation is high due to the greater variance of annual temperature/salinity in the sampling interval. This variability notwithstanding, the mean and standard deviation of the ss morphotypes are similar to the sl morphotypes. To statistically test these comparisons, we chose to perform Welch's *t* test[23] (paired *t* test with unknown and unequal variance) on the ss-sl pairs with no *a priori* assumptions about the variance of the underlying populations[24]. All populations were found to be normal based on a Shapiro-Wilk test[25], except for downcore $\delta^{13}C$ of ss and sl, where we used the non-parametric Mann–Whitney–Wilcoxon ranksum test[26]. From this exercise, we failed to reject the null hypothesis for ss-sl pairs across all archives, that is, the $\delta^{18}O$ and $\delta^{13}C$ difference between ss and sl morphotypes is not statistically significant ($p<0.05$; Table 1). We also pooled all the ss-sl pairs across the different sampling archives and tested for regressions using the maximum likelihood estimate method[27] incorporating bivariate analytical uncertainty[28], where $1\sigma_{analytical} = 0.08‰$ in $\delta^{18}O$, and 0.06‰ in $\delta^{13}C$. Within uncertainty, both $\delta^{18}O$ and $\delta^{13}C$ slopes and intercepts were not significantly different ($p<0.05$) from the 1 : 1 line, where the slope is unity and intercept is zero (Fig. 3).

We use offsets between coeval samples as a metric to statistically compare the ss-sl measurements with the intermediate couplets. The absolute offsets between coeval ss-sl samples ranged from 0–0.52‰ in $\delta^{13}C$ and 0–0.56‰ in $\delta^{18}O$, while the intermediate couplets ranged from 0–0.50‰ in $\delta^{13}C$ and 0.01–0.53‰ in $\delta^{18}O$ (See *Supplementary Table S1* for the range in each archive). The mean ss-sl offset and standard deviations in all archives are not systematic, and closely cluster around zero. We tested for mean ss-sl offsets significantly different from zero using a Student's *t* test in a Monte Carlo framework (n = 5000) to account for analytical error at the ~95% confidence level (i.e. $\pm\ 2\sigma_{analytical}$) incorporated as a Gaussian distribution. All archives failed the test with probabilities ≥70% that both carbon and oxygen stable isotopic offsets were not significantly distinct from zero thus corroborating our initial Welch *t* test outcomes and regression analysis that ss-sl couplets have statistically similar variability in stable isotopic composition.

As the intermediate *G. ruber* (W) pairs are interchangeable amongst coeval couplets (their transitional form inhibits selective categorization), we generated all possible combinations of the couplets in each archive using binomial expansion (See *Methods* for details). Next, we computed the mean (μ_c) and standard deviation (σ_c) of the offsets for each combination. To gain insight into the variability of the intermediate couplets, we report the average mean offset of all the combinations with its associated standard deviation ($<\mu_c> \pm \sigma_\mu$; (b1) and (d1) in Table 2) and the average standard deviation of all the offsets with its associated standard deviation ($<\sigma_c> \pm \sigma_\sigma$; (b2) and (d2) in Table 2) in the binomially generated combinations. We note that the average standard deviation of the intermediate *G. ruber* (W) offset ($<\sigma_c>$), a measure of non-morphotypical variability, is statistically similar to the corresponding mean and standard deviation of the ss-sl offset within analytical error ($p<0.05$; Table 2).

Apart from stable isotope analysis, the sediment trap allows us to quantify the monthly abundance of each morphotype. Over our sampling interval, in general, we observe the sl morphotypes to be more abundant than the other morphotypes. Concerning seasonal preferences, the census data indicate that neither ss, sl, nor the intermediate *G. ruber* (W) specimens prefer any particular season in our sampling window (Fig. 4). Moreover, we found no persistent season where one morphotype dominates over the others.

Ruling out a seasonal bias in morphotype, we investigated whether the ss and sl morphotypes had preferential calcifying depth habitats as suggested in previous studies: ss preferring 0–25 m and sl preferring 25–50 m. To assess the potential for resolving depth-specific signals in marine sediment, we applied INFAUNAL[22] at surface and subsurface depths in the Gulf of Mexico to construct idealized virtual sediment samples for the two habitats. We constructed two 50-year-long pseudo-$\delta^{18}O_{carbonate}$ time series using monthly temperature and salinity from the ECMWF ORA-S4 reanalysis dataset[29] at depths of 5 m (ss) and 55 m (sl; see *Supplementary Fig. 2*). These depths were chosen based on those available in the ORA-S4 dataset that were closest to the extremes of the previously hypothesized calcification depths (we also performed the experiment using 35 m and 45 m depths; see *Methods*). Next, we performed bootstrap Monte Carlo picking experiments (n = 10000) on these virtual sediment samples with 50 pseudo-foraminifera to determine whether the offset produced in INFAUNAL would be comparable to the offset observed in the ss-sl data. We chose 50-year-long time series and 50

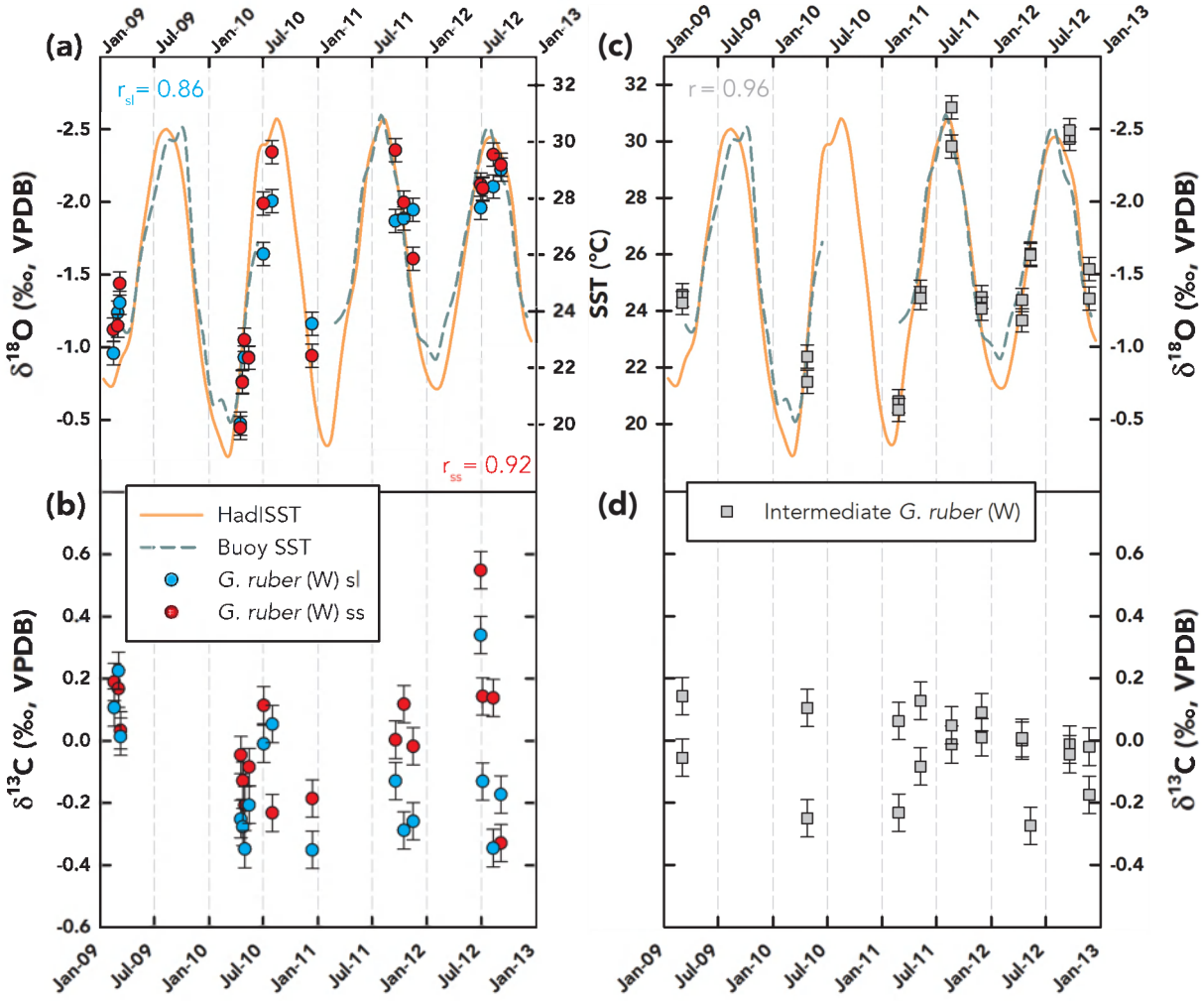

Figure 2 | Stable Isotopic Results from the Sediment Trap. $\delta^{18}O$ (a) and $\delta^{13}C$ (b) of *G. ruber* (W) sl (blue circles) and ss (red circles) morphotypes along with $\delta^{18}O$ (c) and $\delta^{13}C$ (d) of intermediate *G. ruber* (W) morphotypes (gray squares) reported relative to VPDB (‰) with error bars based on analytical precision ($\pm 1\sigma$; $\delta^{18}O$ – 0.08‰ and $\delta^{13}C$ – 0.06‰) over 2009–2013. Sea-surface temperature (SST) from HadISST[40] (orange line) and nearby NDBC Buoy SST (27.795°N, 90.648°W – Green Canyon; green dashed line) over the same time period are plotted in (a) and (c), scaled according to the $\delta^{18}O$ axis, based on the slope from Bemis et al., 1998[41]. Correlation coefficients are calculated with buoy SSTs when available and HadISST-based SSTs when the former are unavailable.

pseudo-foraminifera for the experiment based on approximately equivalent sample resolution and number of foraminifera analyzed in the core-top and downcore samples (the high temporal resolution and abundance of the sediment trap samples does not allow for a one-to-one downcore analog). The INFAUNAL results indicated that 50 foraminifera picked from the 5 m pseudo-$\delta^{18}O_{carbonate}$ time series and 50 from the 55 m time series could resolve these depth-specific signals with a high probability (≥90%) and that the offset between the picked means of the idealized time series was significantly distinct from zero ($p<0.001$). However, this idealized population of offsets is significantly different than the ss-sl offset observed in the core-top and downcore $\delta^{18}O$ data ($p<0.001$), the latter of which is not distinct from zero ($p<0.05$; Fig. 5).

Discussion

Our observations and statistical tests indicate that there are neither significant nor systematic stable isotopic differences between *G. ruber* (W) ss and sl populations across three different sampling archives in the Gulf of Mexico (Fig. 3). The variability in $\delta^{13}C$ and $\delta^{18}O$ of both morphotypes is statistically indistinguishable (Table 1). The intermediate *G. ruber* (W) samples display very similar variability and contain intra-sample variability comparable to the ss-sl populations (Table 2), thereby preventing us from rejecting the geochemical test of the null hypothesis. Taken together, our observations imply that morphotypical variability in *G. ruber* (W) has little if any control on its $\delta^{13}C$ and $\delta^{18}O$ composition.

Though the $\delta^{13}C$ variability in the sediment trap samples is seemingly chaotic, the $\delta^{18}O$ variability is distinctly controlled by climate. Despite steep rates of change in SST during boreal spring and fall at the northern Gulf of Mexico (~10°C seasonal cycle), the $\delta^{18}O$ of both morphotypes in the sediment trap samples reliably capture SSTs (Fig. 2). The same is true for the intermediate couplets. In examining coeval offsets, the $\delta^{18}O$ standard deviation is reduced by ~50% compared to the overall standard deviation of each morphotype (~0.6‰ vs. ~0.2‰; Tables 1 and 2), whereas the overall $\delta^{13}C$ standard deviations are similar to that of the offset (~0.2‰ vs. 0.2‰; Tables 1 and 2). This implies that intra-morphotype $\delta^{13}C$ is as variable as inter-morphotype $\delta^{13}C$, a result that is in line with previous studies highlighting the complex controls on stable isotopic carbon in foraminifera[30,31]. We observe similar variability in the intermediate *G. ruber* (W) couplets (±0.23‰), supporting this interpretation.

What are the ecological implications of our observations concerning the habitat of *G. ruber* (W) morphotypes and its effect on paleoceanographic reconstructions? From our sediment trap flux data, we

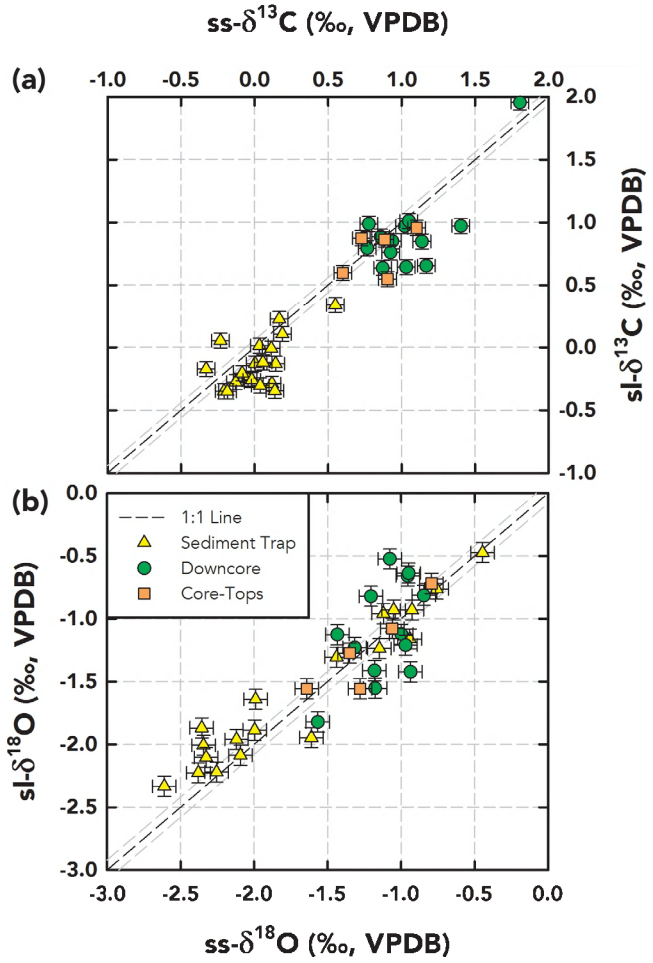

Figure 3 | Regression Analysis of ss-sl Samples Across Three Sampling Archives. *G. ruber* (W) $\delta^{13}C$ (a) and $\delta^{18}O$ (b) results for ss (abscissa) versus sl (ordinate) from the sediment trap (yellow triangles), core-top (orange squares), and downcore samples (green circles) with error bars based on analytical precision ($\pm 1\sigma_{analytical}$; $\delta^{13}C$ – 0.06‰ and $\delta^{18}O$ – 0.08‰). The 1:1 line (black dashed line) along with uncertainty limits (grey dashed lines based on $\pm 1\sigma_{analytical}$) is also plotted. The maximum likelihood regression lines incorporating bivariate uncertainty are: 1) sl-$\delta^{13}C$ = (−0.11 ± 0.06) + (0.96 ± 0.06)*ss-$\delta^{13}C$ and 2) sl-$\delta^{18}O$ = (−0.01 ± 0.05) + (0.96 ± 0.04)*ss-$\delta^{18}O$.

find no evidence that ss, sl, or the intermediate *G. ruber* (W) samples prefer one season over another (Fig. 4). The data also indicate that no particular morphotype is persistently more abundant than any other morphotype. This supports the inference that all morphotypes of *G. ruber* (W) live throughout the year and that paleoceanographic records generated using the species should be representative of annual conditions, substantiating previous studies in the Gulf of Mexico[32,33] and elsewhere[34]. Using INFAUNAL, we show that pseudo-foraminifera calcifying exclusively at 5 m and 55 m can resolve depth-specific $\delta^{18}O$ (temperature and salinity) signals with a very high probability (≥90% with 50 specimens in 50-year sample resolution and ≥70% at 45 m; See *Methods* and *Supplementary Fig. 3*). We also show that the resulting distribution of pseudo-foraminifera is significantly different from our core-top and downcore data, which is centered on zero (Fig. 5). This result implies that ss and sl morphotypes must dwell and migrate to similar depths in the Gulf of Mexico. We infer that these depths are restricted to the upper portion of the mixed layer due to the excellent correlation between both morphotypes and SST in the sediment trap samples (r_{ss} = 0.92, r_{sl} = 0.86; Fig. 2). Thus, our observations and modeling results

Table 1 | Mean and Standard Deviation of ss-sl Isotopic Measurements in Each Sampling Archive with Outcomes of Welch's *t* test at $p<0.05$ level, where H = H_o implies null hypothesis cannot be rejected; H = H_a implies null hypothesis can be rejected

	Sediment Trap	Core-Tops	Downcore
No. of Pairs	17	5	13
$\delta^{18}O_{ss}$ (‰)	−1.58 ± 0.64	−1.22 ± 0.32	−1.12 ± 0.21
$\delta^{18}O_{sl}$ (‰)	−1.50 ± 0.56	−1.24 ± 0.35	−1.10 ± 0.39
H	H_o	H_o	H_o
$\delta^{13}C_{ss}$ (‰)	0.01 ± 0.21	0.84 ± 0.19	1.06 ± 0.28
$\delta^{13}C_{sl}$ (‰)	−0.12 ± 0.21	0.77 ± 0.18	0.92 ± 0.34
H	H_o	H_o	H_o*

*- H = H_o based on Mann–Whitney–Wilcoxon due to the non-parametric nature of underlying populations.

unequivocally indicate that *G. ruber* (W)-based paleoceanographic records, regardless of morphotype, reflect annual surface water conditions in the Gulf of Mexico.

Contrary to previous *G. ruber* (W)-morphotype studies based on core-tops and downcore samples in the South China Sea and Japanese seas[16–19], our findings suggest no morphotype-based biases in utilizing a non-selective mixture of *G. ruber* (W) ss and sl for paleoceanographic reconstructions. Nevertheless, our findings are corroborated by studies utilizing sediment traps in the Indo-Pacific seas[20] and plankton tow samples around Japan[35], where no geochemical and flux differences were observed in the former and sea-surface maxima in abundance for both morphotypes were observed in the plankton tows. We feel that this inconsistency may arise either due to the influence of the large latitudinal extent of sample selection in the previous studies resulting in dissimilar seasonal cycles across all the sampling locations, loose temporal constraints on core-tops and/or possibly from limited sample numbers, few specimens analyzed per sample, and a non-rigorous treatment of uncertainty. For example, we note that the core-top samples from the South China Sea in an early study[16] are obtained from a large latitudinal transect spanning from 6°N-22°N where the seasonal cycle changes from a tropical (smaller seasonal cycle) to sub-tropical (larger seasonal cycle) setting. The thermocline and other oceanographic features are variable over this latitudinal range as well[36,37]. Quantifying these multiple sources of uncertainty in the South China/Japanese Sea and focusing solely on ss-sl-based isotopic variability is non-trivial and outside the scope of this work, thereby limiting a one-to-one comparison with our results. Further, the size fraction of specimens used in our study (212–300 μm) is smaller than earlier studies (315–400 μm[16], 250–350 μm[18]) adding another barrier in directly comparing these studies, as size and ontogeny can significantly affect $\delta^{13}C$ and $\delta^{18}O$ variability[38,39]. Though preliminary sediment trap work in the South China Sea region is equivocal about the two morphotypes[21], a more comprehensive spatially-invariant sediment trap/plankton tow study would certainly assist in interpreting the earlier core-top/downcore studies[16–19].

In summary, we demonstrate the advantage and application of using a comprehensive dataset in tandem with a forward modeling statistical approach to glean insights into ecological variability. Such data-model comparisons characterized with robust uncertainty constraints are useful in discerning the effect of ecological parameters on paleoceanographic reconstructions. In this study, we show that all lines of evidence (observations, null hypothesis testing, and data-model comparisons) indicate that *G. ruber* (W) ss, sl, and intermediate morphotypes live throughout the year and dwell in the upper portion of the mixed layer in the Gulf of Mexico. Hence, downcore reconstructions using non-selective mixtures of *G. ruber* (W) specimens should reflect annual surface water conditions.

Table 2 | Mean and Standard Deviation (1σ) of Offsets Between Coeval ss-sl Samples (a and c) and Corresponding Mean (b1 and d1), Standard Deviation (b2 and d2), and their Standard Deviation for all Combinations of Intermediate *G. ruber* (W) Couplets

		Sediment Trap	Core-Tops	Downcore
$<\Delta\delta^{18}O_{ss\text{-}sl}>$ (‰)	(a) $\mu_{ss\text{-}sl} \pm \sigma_{ss\text{-}sl}$	−0.08 ± 0.20	0.01 ± 0.15	−0.02 ± 0.33
	(b1) $<\mu_c> \pm \sigma_\mu$	0.01 ± 0.04	−0.02 ± 0.06	0 ± 0.07
$<\Delta\delta^{18}O_{Null}>$ (‰)	±	±	±	±
	(b2) $<\sigma_c> \pm \sigma_\sigma$	0.14 ± 0.01	0.14 ± 0.02	0.26 ± 0.01
$<\Delta\delta^{13}C_{ss\text{-}sl}>$ (‰)	(c) $\mu_{ss\text{-}sl} \pm \sigma_{ss\text{-}sl}$	0.13 ± 0.18	0.07 ± 0.18	0.14 ± 0.22
	(d1) $<\mu_c> \pm \sigma_\mu$	−0.02 ± 0.07	0.03 ± 0.08	0.01 ± 0.08
$<\Delta\delta^{13}C_{Null}>$ (‰)	±	±	±	±
	(d2) $<\sigma_c> \pm \sigma_\sigma$	0.23 ± 0.02	0.18 ± 0.02	0.29 ± 0.02

Methods

Specimen Selection. We chose *G. ruber* (W) sensu stricto (ss) and sensu lato (sl) specimens in the 212–300 μm size fraction for all sampling archives. Sensu lato (Fig. 1 a and b) was characterized as a kummerform having three compressed spherical chambers in the final whorl where the final chamber was smaller and flattened compared to the others, forming a moderate to high trochospiral form, with a rounded primary aperture situated asymmetrically over the previous suture. Sensu stricto (Fig. 1 c and d) was characterized as having three spherical chambers in the final whorl that progressively increased in size and had a moderate trochospire shape, with radial sutures containing supplementary apertures and a primary aperture that was wide and more arched than the sl morphotype, symmetric over the previous suture. Intermediate specimens include tests with morphotypical variability transitional to that between ss and sl (for example, a normalform containing compressed chambers in the final whorl and a wide, highly-arched primary aperture that sat asymmetrically over the previous suture or a normalform containing a narrow, rounded, primary aperture sitting symmetrically over the previous suture, with depressed radial sutures with ancillary suture apertures).

Stable Isotope Analysis. We selected 6–20 specimens of each *G. ruber* (W) morphotype from the sediment trap samples and ≥50 specimens for the downcore/core-top samples. Specimens were crushed and homogenized, and cleaned with methanol before geochemical analysis. Stable isotopes were measured using a Thermo-Finnigan MAT 253™ isotope ratio mass spectrometer coupled to a Kiel IV Carbonate Device housed in the Analytical Laboratory for Paleoclimate Studies (ALPS) at the Jackson School of Geosciences, University of Texas at Austin. The 1σ precision of the stable isotopic measurements in this study based on multiple analyses of an in-house carbonate standard (n = 28) is 0.03‰ for $\delta^{13}C$ and 0.06‰ for $\delta^{18}O$, consistent with the long-term precision for this instrumental setup (0.06‰ for $\delta^{13}C$ and 0.08‰ for $\delta^{18}O$). All stable isotope values are reported relative to Vienna Pee Dee Belemnite (VPDB) in standard notation.

Year-normalized Flux. We calculated year-normalized flux (Fig. 4) from the sediment trap using:

$$\frac{Monthly\ count\ of\ particular\ morphotype}{Yearly\ total\ of\ all\ morphotypes} \times 100\% \quad (1)$$

Binomial Expansion for Intermediate Couplet Combinations. While computing the mean and standard deviation of the offsets between coeval intermediate pairs for an archive, we considered all possible combinations by interchanging samples of the intermediate couplets. In offset space, this effectively reduces to a change in sign before computing the mean and standard deviation of all the offsets in an archive, thereby following a binary 'on-off' pattern. The number of unique combinations n possible for a given number of samples s in an archive is obtained by binomial expansion:

$$n = 2^{s-1} + 1 \quad (2)$$

After generating n combinations, we computed the mean (μ_c) and standard deviation (σ_c) of the offsets for each combination. We report the average mean offset of all the combinations with its associated standard deviation ($<\mu_c> \pm \sigma_\mu$; (b1) and (d1) in Table 2) and the average standard deviation of all the offsets with its associated standard deviation ($<\sigma_c> \pm \sigma_\sigma$; (b2) and (d2) in Table 2) in the binomially generated combinations to compare the variability of offsets in the intermediate couplets and compare them to the ss-sl offsets.

INFAUNAL model. Bootstrap Monte Carlo simulations (n = 10000) were performed to generate a population of means that incorporated analytical uncertainty (±2σ) and sampling uncertainty involved with utilizing 50 pseudo-foraminifera in a virtual sediment sample representing 50 years using the Individual Foraminiferal Approach Uncertainty Analysis (INFAUNAL) model for multi-test foraminiferal analysis as described by Thirumalai et al. (2013)[22]. We applied the algorithm to

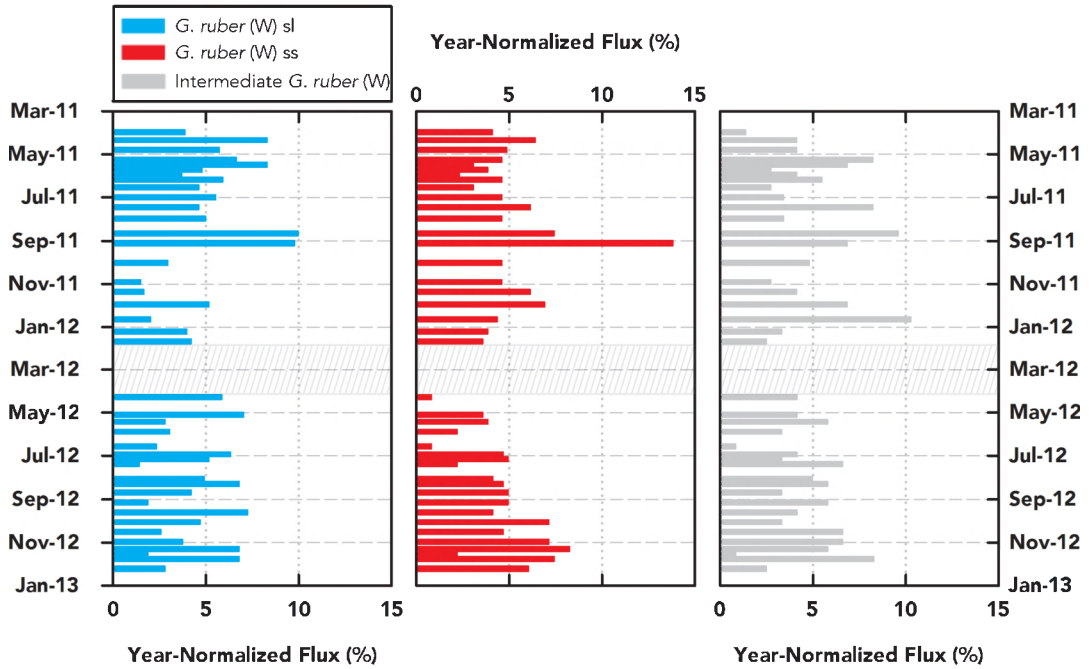

Figure 4 | Year-Normalized Flux. Sediment trap-based year-normalized flux (%) measurements for *G. ruber* (W) sl (blue), ss (red), and intermediate (grey) morphotypes. Persistent seasonal preferences or abundance of one morphotype over another are not observed. Box containing hatched lines indicates a gap in data collection.

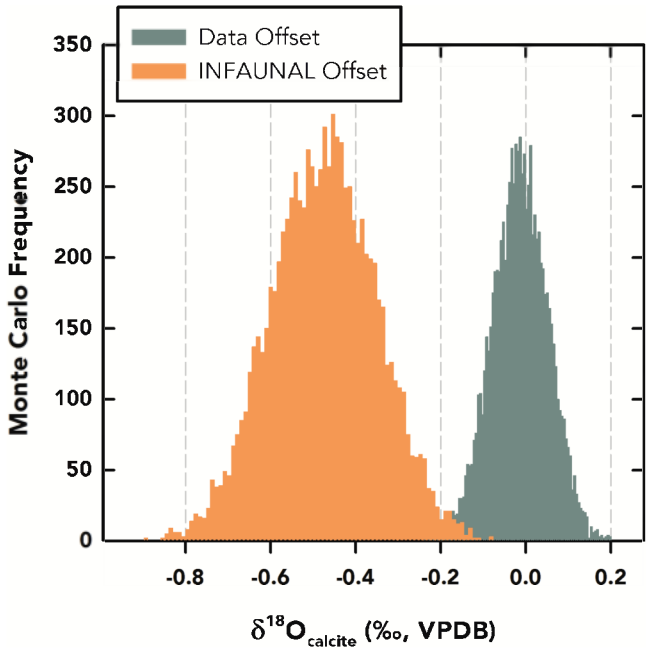

Figure 5 | Data-Model Comparison of Simulated Offsets with Uncertainty Constraints. Monte-Carlo-based histogram of mean offsets from the ss-sl data (green) in core-top/downcore samples compared to a histogram of mean offsets between pseudo-$\delta^{18}O$ time series from 5 m and 55 m depth generated using INFAUNAL[22] (orange). Both populations incorporate analytical and sampling uncertainty and are significantly different from each other ($p<0.001$). Note that the model-offset population is significantly distinct from zero ($p<0.001$) while the data-offset population is not different from zero ($p<0.05$).

perform picking experiments on a $\delta^{18}O$ time series generated from temperature and salinity data at depths of 5 m and 55 m using the ECMWF ORA-S4 ocean reanalysis dataset[29] with data extracted from 26.7°N, 93.9°W (the location of our core-top and downcore samples) in the Gulf of Mexico. 5 and 55 m depths were chosen from the reanalysis dataset because they were the closest to the extremes of the previously hypothesized calcification depths (0–25 m for ss and 25–50 m for sl). To ensure the robustness of these results, we also performed the same INFAUNAL picking experiments at 35 m and 45 m (*Supplementary Fig. 3*). Similar to the resulting offsets between 5 and 55 m, we observed that there was a high probability (≥70%) that pseudo-foraminifera calcifying at 5 m versus 45 m can resolve depth-specific $\delta^{18}O$ signals. The probability of resolving depth-specific signals using idealized pseudo-foraminifera became lower at 35 m (≥25%), limiting our ability to test hypothesis of selective ss-sl calcification depths using a model-data comparison. However, all offsets produced by INFAUNAL between 5 and 35 m, 45 m, and 55 m are still significantly distinct from zero ($p<0.001$) and from the $\delta^{18}O$ data ($p<0.001$), the latter of which is not significantly different from zero (we also tested this at 100 and 5000 Monte Carlo simulations and obtained the same outcome). This indicates that it is statistically unlikely that most ss and sl specimens are calcifying deeper than 35 m. Furthermore, since the mixed layer at the sediment trap site extends well beyond 55 m for most months of the year (*Supplementary Fig. 4*), our results hold that both *G. ruber* (W) morphotypes in the northern Gulf of Mexico calcify in the upper portion of the mixed layer.

1. Richey, J. N., Poore, R. Z., Flower, B. P. & Quinn, T. M. 1400 yr multiproxy record of climate variability from the northern Gulf of Mexico. *Geol* **35**, 423 (2007).
2. Mohtadi, M. *et al.* North Atlantic forcing of tropical Indian Ocean climate. *Nature* **509**, 76–80 (2014).
3. LoDico, J. M., Flower, B. P. & Quinn, T. M. Subcentennial-scale climatic and hydrologic variability in the Gulf of Mexico during the early Holocene. *Paleoceanography* **21**, PA3015 (2006).
4. Poore, R. Z., Dowsett, H. J., Verardo, S. & Quinn, T. M. Millennial- to century-scale variability in Gulf of Mexico Holocene climate records. *Paleoceanography* **18**, 1048 (2003).
5. Spero, H. J., Mielke, K. M., Kalve, E. M., Lea, D. W. & Pak, D. K. Multispecies approach to reconstructing eastern equatorial Pacific thermocline hydrography during the past 360 kyr. *Paleoceanography* **18**, 1022 (2003).
6. Ganssen, G. *et al.* Quantifying sea surface temperature ranges of the Arabian Sea for the past 20 000 years. *Clim. Past Discuss.* **6**, 2795–2814 (2010).
7. Weldeab, S., Lea, D. W., Oberhänsli, H. & Schneider, R. R. Links between southwestern tropical Indian Ocean SST and precipitation over southeastern Africa over the last 17 kyr. *Palaeogeogr. Palaeoclimatol. Palaeoecol.* **410**, 1–13 (2014).
8. Robbins, L. L. & Healy-Williams, N. Toward a classification of planktonic foraminifera based on biochemical, geochemical, and morphological criteria. *J Foram Res* **21**, 159–167 (1991).
9. Srinivasan, M. S., Kennett, J. P. & Bé, A. W. *Globorotalia menardii neoflexuosa* new subspecies from the northern Indian Ocean. *Deep-sea Res* **21**, 321–324 (1974).
10. Schmidt, G. A. & Mulitza, S. Global calibration of ecological models for planktic foraminifera from coretop carbonate oxygen-18. *Mar Micropaleontol* **44**, 125–140 (2002).
11. Farmer, E. C., Kaplan, A., de Menocal, P. B. & Lynch-Stieglitz, J. Corroborating ecological depth preferences of planktonic foraminifera in the tropical Atlantic with the stable oxygen isotope ratios of core top specimens. *Paleoceanography* **22**, PA3205 (2007).
12. d'Orbigny, A. D. Tableau méthodique de la classe des Céphalopodes. *Annales des Sciences Naturelles* **7**, 245–314 (1826).
13. Van den Broeck, E. Etude sur les Foraminiferes de la Barbade (Antilles). *Ann. Soc. Belge Microsc* **1**, 55–152 (1876).
14. Galloway, J. J. & Wissler, S. G. Pleistocene foraminifera from the Lomita Quarry, Palos Verdes Hills, California. *J Paleontol* 35–87 (1927).
15. d'Orbigny, A. in *Histoire physique, politique et naturelle de l'île de Cuba* (La Sagra, de, R.) 1–224 (Bertrand, 1839).
16. Wang, L. Isotopic signals in two morphotypes of *Globigerinoides ruber* (white) from the South China Sea: implications for monsoon climate change during the last glacial cycle. *Palaeogeogr. Palaeoclimatol. Palaeoecol.* **161**, 381–394 (2000).
17. Löwemark, L., Hong, W.-L., Yui, T.-F. & Hung, G.-W. A test of different factors influencing the isotopic signal of planktonic foraminifera in surface sediments from the northern South China Sea. *Mar Micropaleontol* **55**, 49–62 (2005).
18. Steinke, S. *et al.* Mg/Ca ratios of two Globigerinoides ruber(white) morphotypes: Implications for reconstructing past tropical/subtropical surface water conditions. *Geochem. Geophys. Geosyst.* **6**, Q11005 (2005).
19. Kawahata, H. Stable isotopic composition of two morphotypes of Globigerinoides ruber (white) in the subtropical gyre in the North Pacific. *Paleontol Res* **9**, 27–35 (2005).
20. Mohtadi, M. *et al.* Low-latitude control on seasonal and interannual changes in planktonic foraminiferal flux and shell geochemistry off south Java: A sediment trap study. *Paleoceanography* **24**, PA1201 (2009).
21. Lin, H.-L., Wang, W.-C. & Hung, G.-W. Seasonal variation of planktonic foraminiferal isotopic composition from sediment traps in the South China Sea. *Mar Micropaleontol* **53**, 447–460 (2004).
22. Thirumalai, K., Partin, J. W., Jackson, C. S. & Quinn, T. M. Statistical constraints on El Niño Southern Oscillation reconstructions using individual foraminifera: A sensitivity analysis. *Paleoceanography* **28**, 401–412 (2013).
23. Welch, B. L. The Generalization of Students Problem When Several Different Population Variances Are Involved. *Biometrika* **34**, 28–35 (1947).
24. Ruxton, G. D. The unequal variance t-test is an underused alternative to Student's t-test and the Mann-Whitney U test. *Behav Ecol* **17**, 688–690 (2006).
25. Shapiro, S. S. & Wilk, M. B. An Analysis of Variance Test for Normality (Complete Samples). *Biometrika* **52**, 591–& (1965).
26. Mann, H. B. & Whitney, D. R. On a test of whether one of two random variables is stochastically larger than the other. *Ann Math Stat* **18**, 50–60 (1947).
27. York, D., Evensen, N. M., Martínez, M. L. & De Basabe Delgado, J. Unified equations for the slope, intercept, and standard errors of the best straight line. *Am. J. Phys.* **72**, 367 (2004).
28. Thirumalai, K., Singh, A. & Ramesh, R. A MATLAB™ code to perform weighted linear regression with (correlated or uncorrelated) errors in bivariate data. *J Geol Soc India* **77**, 377–380 (2011).
29. Balmaseda, M. A., Mogensen, K. & Weaver, A. T. Evaluation of the ECMWF ocean reanalysis system ORAS4. *Q.J.R. Meteorol. Soc.* (2012).
30. Spero, H. J. & Williams, D. F. Opening the carbon isotope 'vital effect' black box 1. Seasonal temperatures in the euphotic zone. *Paleoceanography* **4**, 593–601 (1989).
31. Spero, H. J., Bijma, J., Lea, D. W. & Bemis, B. E. Effect of seawater carbonate concentration on foraminiferal carbon and oxygen isotopes. *Nature* **390**, 497–500 (1997).
32. Spear, J. W. & Poore, R. Z. *Seasonal Flux and Assemblage Composition of Planktic Foraminifera from the Northern Gulf of Mexico, 2008-2009.* 1–17 (US Geological Survey Open File Report, 2011).
33. Poore, R. Z., Tedesco, K. A. & Spear, J. W. Seasonal Flux and Assemblage Composition of Planktic Foraminifers from a Sediment-Trap Study in the Northern Gulf of Mexico. *J Coastal Res* 6–19 (2013).
34. Deuser, W. G. Seasonal variations in isotopic composition and deep-water fluxes of the tests of perennially abundant planktonic foraminifera of the Sargasso Sea; results from sediment-trap collections and their paleoceanographic significance. *J Foram Res* **17**, 14–27 (1987).
35. Kuroyanagi, A. & Kawahata, H. Vertical distribution of living planktonic foraminifera in the seas around Japan. *Mar Micropaleontol* **53**, 173–196 (2004).
36. Qu, T., Mitsudera, H. & Yamagata, T. Intrusion of the North Pacific waters into the South China Sea. *J. Geophys. Res.* **105**, 6415–6424 (2000).

37. Liu, Q., Jia, Y., Liu, P., Wang, Q. & Chu, P. C. Seasonal and Intraseasonal Thermocline Variability in the Central South China Sea. *Geophysical Research Letters* **28**, 4467–4470 (2007).
38. Sarkar, A., Ramesh, R. & Bhattacharya, S. K. Effect of sample pretreatment and size fraction on the $\delta^{18}O$ and $\delta^{13}C$ values of foraminifera in Arabian Sea sediments. *Terra Nova* **2**, 488–493 (1990).
39. Peeters, F. J., Brummer, G.-J. A. & Ganssen, G. The effect of upwelling on the distribution and stable isotope composition of *Globigerina bulloides* and *Globigerinoides ruber* (planktic foraminifera) in modern surface waters of the NW Arabian Sea. *Global and Planetary Change* **34**, 269–291 (2002).
40. Rayner, N. A. *et al.* Global analyses of sea surface temperature, sea ice, and night marine air temperature since the late nineteenth century. *J. Geophys. Res.* **108**, 4407 (2003).
41. Bemis, B. E., Spero, H. J., Bijma, J. & Lea, D. W. Reevaluation of the oxygen isotopic composition of planktonic foraminifera: Experimental results and revised paleotemperature equations. *Paleoceanography* **13**, 150–160 (1998).

Acknowledgments

We thank the crew of the R/V Pelican for assisting us in the collection and redeployment of the sediment trap, and the crew of the R/V Cape Hatteras for aid in obtaining the cores utilized in this study. We acknowledge Caitlin Reynolds for aiding sample preparation and Jennifer Flannery for help with the SEM images. The authors are thankful to Judson Partin for helpful discussion and for critiquing a preliminary draft of this manuscript along with Deb Willard. K. T. thanks the UTIG Ewing-Worzel fellowship for support. This research was funded by the U.S. Geological Survey Climate and Land Use Research & Development program and the National Science Foundation (OCE-0902921). This is UTIG Contribution #2719.

Author contributions

K.T., J.N.R., T.M.Q. and R.Z.P. conceived the study and interpreted the results. J.N.R. and K.T. acquired all the data involved in the study and produced the supplementary text. K.T. performed the modeling and statistical analysis, wrote the manuscript, and generated the figures and tables in the main text.

Additional information

Supplementary information accompanies this paper at http://www.nature.com/scientificreports

Competing financial interests: The authors declare no competing financial interests.

How to cite this article: Thirumalai, K., Richey, J.N., Quinn, T.M. & Poore, R.Z. *Globigerinoides ruber* morphotypes in the Gulf of Mexico: A test of null hypothesis. *Sci. Rep.* **4**, 6018; DOI:10.1038/srep06018 (2014).